JOC Article

Novel Photoswitchable Receptors: Synthesis and Cation-Induced Self-Assembly into Dimeric Complexes Leading to Stereospecific [2+2]-Photocycloaddition of Styryl Dyes Containing a 15-Crown-5 Ether Unit

Sergey P. Gromov,*[,†] Evgeny N. Ushakov,[‡] Olga A. Fedorova,[†] Igor I. Baskin,[§] Alexei V. Buevich,[∥] Elena N. Andryukhina,[†] Michael V. Alfimov,[†] Dan Johnels,[⊥] Ulf G. Edlund,[⊥] James K. Whitesell,[▽] and Marye Anne Fox*[,▽]

Photochemistry Center of the Russian Academy of Sciences, 7a ul. Novatorov, Moscow 119421, Russia, Institute of Problems of Chemical Physics, Russian Academy of Sciences, Chernogolovka, Moscow Region 142432, Russia, and N. D. Zelinsky Institute of Organic Chemistry, Russian Academy of Sciences, 47 Leninsky prosp., Moscow 117913, Russia, Wright-Rieman Labs, Rutgers University, Piscataway, New Jersey 08855-0939, Department of Organic Chemistry, Umeå University, Umeå SE-901 87, Sweden, and Department of Chemistry, North Carolina State University, Raleigh, North Carolina 27695-8204

mafox@ncsu.edu

Received April 11, 2003

Styryl dyes **4a**−**e** containing a 15-crown-5 ether unit and a quinoline residue with a sulfonatoalkyl or sulfonatobenzyl *N*-substituent were synthesized. The relationship between the photochemical behavior of these dyes and their aggregates derived from complexation with Mg^{2+} in MeCN was studied using ^{1}H NMR and absorption spectroscopy. The *E*-isomers of **4a**−**e** were shown to form highly stable dimeric (2:2) complexes with Mg^{2+}. Upon irradiation with visible light, the dimeric complexes undergo two competing photoreactions, viz., geometric $E \rightarrow Z$ isomerization, resulting in an anion-capped 1:1 complex of the *Z*-isomer with Mg^{2+} and stereospecific *syn*-head-to-tail [2+2]-cycloaddition, affording a single isomer of bis-crown-containing cyclobutane. The *N*-substituent in the dye has a dramatic effect on the photochemical behavior of the dimeric complex. Molecular dynamics and semiempirical quantum-chemical calculations were carried out to interpret the observed photocycloaddition in the dimer. Conformational equilibria for the dimer of (*E*)-**4b** were analyzed using ^{1}H NMR spectroscopy.

Introduction

Self-assembled multicomponent structures[1−4] containing photoresponsive units[5−9] constitute a series of simple photoswitchable molecular devices.[10−13] Multiphotochromic complexes are of interest as elements of such devices, because of their ability to undergo different types of reversible photoreactions.[14,15] Previously we have reported the synthesis and characterization of photochromic complexes composed of a styryl dye and a crown ether to which various metal ions could be bound.[16−21] The

† Photochemistry Center of the Russian Academy of Sciences.
‡ Institute of Problems of Chemical Physics, Russian Academy of Sciences.
§ N. D. Zelinsky Institute of Organic Chemistry, Russian Academy of Sciences.
∥ Rutgers University.
⊥ Umeå University.
▽ North Carolina State University.

(1) Lindsey, J. S. *New J. Chem*. **1991**, *15*, 153−180.
(2) Lawrence, D. S.; Jiang, T.; Levett, M. *Chem. Rev*. **1995**, *95*, 2229−2260.
(3) Belohradsky, M.; Raymo, F. M.; Stoddart, J. F. *Collect. Czech. Chem. Commun*. **1996**, *61*, 1−43.
(4) Linton, B.; Hamilton, A. D. *Chem. Rev*. **1997**, *97*, 1669−1680.
(5) Shinkai, S. In *Cation Binding by Macrocycles. Complexation of Cationic Species by Crown Ethers*; Inoue, Y., Gokel, G. W., Eds.; Marcel Dekker Inc.: New York, 1990; Chapter 9, pp 397−428.
(6) Pietraszkiewicz, M. In *Comprehensive Supramolecular Chemistry*; Reinhoudt, D. N., Ed.; Pergamon: Oxford, 1996; Vol. 10, pp 225−265.
(7) de Silva, A. P.; Gunaratne, H. Q. N.; Gunnlaugsson, T.; Huxley, A. J. M.; McCoy, C. P.; Rademacher, J. T.; Rice, T. E. *Chem. Rev*. **1997**, *97*, 1515−1566.
(8) Alfimov, M. V.; Gromov, S. P. In *Applied Fluorescence in Chemistry, Biology, and Medicine*; Rettig, W., Strehmel, B., Schrader, S., Seifert, H., Eds.; Springer-Verlag: Berlin, 1999; pp 161−178.
(9) Valeur, B.; Leray, I. *Coord. Chem. Rev*. **2000**, *205*, 3−40.
(10) Lehn, J.-M. *Supramolecular Chemistry. Concepts and Perspectives*; VCH: Weinheim, Germany, 1995; Chapter 8.
(11) Balzani, V.; Scandola, F. In *Comprehensive Supramolecular Chemistry*; Lehn, J.-M., Ed.; Pergamon Press: New York, 1996; Vol. 10, pp 687−746.
(12) Kimura, K. *Coord. Chem. Rev*. **1996**, *148*, 41−61.
(13) Gromov, S. P.; Alfimov, M. V. *Izv. Akad. Nauk, Ser. Khim*. **1997**, 641−665; *Russ. Chem. Bull. (Engl. Transl.)* **1997**, *46*, 611−636.
(14) *Photochromism: Molecules and Systems*; Dürr, H., Bouas-Laurent, H., Eds.; Elsevier: Amsterdam, 1990.
(15) *Organic Photochromic and Thermochromic Compounds*; Crano, J. C., Guglielmetti, R. J., Eds.; Plenum Press: New York, 1999; Vol. 1.
(16) Gromov, S. P.; Fomina, M. V.; Ushakov, E. N.; Lednev, I. K.; Alfimov, M. V. *Dokl. Akad. Nauk SSSR* **1990**, *314*, 1135−1138; *Dokl. Chem. (Engl. Transl.)* **1990**, *314*, 279−282.
(17) Gromov, S. P.; Fedorova, O. A.; Alfimov, M. V. *Mol. Cryst. Liq. Cryst*. **1994**, *246*, 183−186.
(18) Gromov, S. P.; Fedorova, O. A.; Ushakov, E. N.; Buevich, A. V.; Alfimov, M. V. *Izv. Akad. Nauk, Ser. Khim*. **1995**, 2225−2230; *Russ. Chem. Bull. (Engl. Transl.)* **1995**, *44*, 2131−2136.
(19) Gromov, S. P.; Levin, D. E.; Burshtein, K. Y.; Krasnovskii, V. E.; Dmitrieva, S. N.; Golosov, A. A.; Alfimov, M. V. *Izv. Akad. Nauk, Ser. Khim*. **1997**, 999−1006; *Russ. Chem. Bull. (Engl. Transl.)* **1997**, *46*, 959−966.

10.1021/jo034460x CCC: $25.00
Published on Web 06/27/2003

SCHEME 1

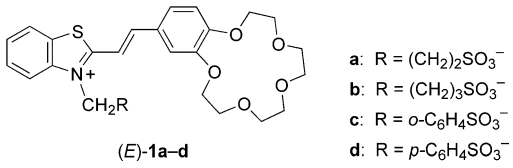

(*E*)-**1a–d**

SCHEME 2

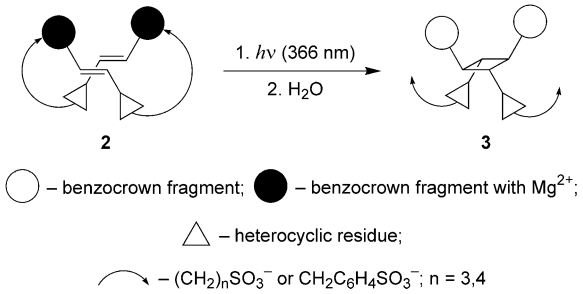

crown-containing styryl dyes bearing a tethered sulfonate anion, such as **1a**−**d** (Scheme 1), were found to be most promising as photoswitchable chelating ligands, in part because of their high solubility in polar solvents. The affinity of **1a**−**d** for alkaline-earth-metal cations significantly increases upon photoinduced $E \rightarrow Z$ isomerization around the central C═C bond, because the geometry of the *Z*-isomer, unlike the initial *E*-isomer, allows *intramolecular* ion pairing of the sulfonate anion with the crowned metal cation.[22−24]

In the presence of Mg^{2+}, the *E*-isomers of **1a**−**d** were found to aggregate into dimeric metal complexes **2** through two-center *intermolecular* ion pairing,[25,26] Scheme 2. The dye molecules in these complexes can undergo not only $E \rightarrow Z$ photoisomerization but also stereospecific *anti*-head-to-tail [2+2]-photocycloaddition (PCA) to produce a single cyclobutane isomer, **3**.[25] The quantum yield of PCA depends strongly on both the length and flexibility of the *N*-substituent in the benzothiazole residue, although the cycloadduct configuration remains unchanged in the series.

We suggested that the relative orientation of the two reacting C−C═C−C fragments in the dimeric complex and, hence, the configuration of the final product of PCA could be controlled by varying the structure of the heterocyclic residue in the dye. Molecular mechanics simulations performed for dimeric complexes of various metal ion-capped crown-containing styryl dyes[27,28] predict a *syn*-head-to-tail pattern of PCA in dyes containing a quinoline residue. To test this prediction, we synthesized the crown-containing styrylquinoline dyes **4a**−**g** and studied the relationship between their photochemical behavior and complex formation with Mg^{2+} in MeCN.

Results and Discussion

Synthesis. The styryl dyes **4a**−**e** were synthesized in 54−99% yields by quaternization of the crown-containing 4-styrylquinoline **5** by appropriate reactants, i.e., **6a**−**e** (Scheme 3).

Compound **5** was prepared by condensation of 4-methylquinoline with 4′-formylbenzo-15-crown-5 ether (**7**) (Scheme 4). NaOMe was used, as base, to promote this reaction.

We expected that NaOMe would facilitate the condensation of 4-methylquinoline with **7** by deprotonation of the methyl group of 4-methylquinoline, thus providing an anionic nucleophile, and by activating the formyl group of **7** by binding Na^+ to the crown ether moiety. In the presence of NaOMe, the condensation readily occurred at ambient temperature, but the yield of **5** was low (12%), presumably because the base also promoted the regioselective Michael-like reaction between **5** and 4-methylquinoline, yielding bisheterocyclic compound **8** (63%). The yield of **8** remained substantial even with an excess of **7** over 4-methylquinoline. To avoid the formation of **8**, other reaction conditions were tested. When the amount of NaOMe in the reaction mixture was decreased, and $NaClO_4$ was added to activate the formyl derivative **7** through complex formation, the yield of **8** diminished to 2%, while the yield of **5** increased to 28%.

Dye **4f** was synthesized by condensation of compound **7** with *N*-ethyl-4-methylquinolinium iodide (**9**) in the presence of pyridine (Scheme 5). The dye **4g** was obtained by addition of excess perchloric acid to **4f**.

The structures of the resulting compounds **4a**−**g**, **5**, and **8** were confirmed by ^1H NMR spectroscopy. The spin−spin coupling constants for the olefinic protons of **4a**−**g** (15.6−15.8 Hz) point to a *trans*-double bond in these dyes. The purity of **4a**−**e** was analyzed by reversed-phase HPLC (Supporting Information).

Complexation and Photochemical Behavior of Dyes 4a−**e.** The absorption spectra for dyes (*E*)-**4a**−**e** in MeCN in the absence/presence of $Mg(ClO_4)_2$ are summarized in Table 1. The absorption spectra of (*E*)-**4a**−**c** have very similar profiles with a broad long-wavelength band in the 400−500 nm region, as illustrated in Figure 1 for **4e** and Figure 2 for **4a**. For the dyes (*E*)-**4d**,**e** containing a sulfonatobenzyl group, the long-wavelength maxima are shifted bathochromically by 5−9 nm relative to those for (*E*)-**4a**−**c**, which bear a more flexible alkyl sulfonate. In the presence of $Mg(ClO_4)_2$, all of the dyes show a large hypsochromic shift of their long-wavelength absorption bands (37−42 nm), presumably

(20) Gromov, S. P.; Ushakov, E. N.; Fedorova, O. A.; Soldatenkova, V. A.; Alfimov, M. V. *Izv. Akad. Nauk, Ser. Khim.* **1997**, 1192−1197; *Russ. Chem. Bull. (Engl. Transl.)* **1997**, *46*, 1143−1148.
(21) Alfimov, M. V.; Churakov, A. V.; Fedorov, Y. V.; Fedorova, O. A.; Gromov, S. P.; Hester, R. E.; Howard, J. A. K.; Kuz'mina, L. G.; Lednev, I. K.; Moore, J. N. *J. Chem. Soc., Perkin Trans. 2* **1997**, 2249−2256.
(22) Alfimov, M. V.; Gromov, S. P.; Lednev, I. K. *Chem. Phys. Lett.* **1991**, *185*, 455−460.
(23) Barzykin, A. V.; Fox, M. A.; Ushakov, E. N.; Stanislavsky, O. B.; Gromov, S. P.; Fedorova, O. A.; Alfimov, M. V. *J. Am. Chem. Soc.* **1992**, *114*, 6381−6385.
(24) Gromov, S. P.; Golosov, A. A.; Fedorova, O. A.; Levin, D. E.; Alfimov, M. V. *Izv. Akad. Nauk, Ser. Khim.* **1995**, 129−135; *Russ. Chem. Bull. (Engl. Transl.)* **1995**, *44*, 124−130.
(25) Gromov, S. P.; Fedorova, O. A.; Ushakov, E. N.; Baskin, I. I.; Lindeman, A. V.; Malysheva, E. V.; Balashova, T. A.; Arsen'ev, A. S.; Alfimov, M. V. *Akad. Nauk, Ser. Khim.* **1998**, 99−107; *Russ. Chem. Bull. (Engl. Transl.)* **1998**, *47*, 97−106.
(26) Ushakov, E. N.; Gromov, S. P.; Buevich, A. V.; Baskin, I. I.; Fedorova, O. A.; Vedernikov, A. I.; Alfimov, M. V.; Eliasson, B.; Edlund, U. *J. Chem. Soc., Perkin Trans. 2* **1999**, 601−607.
(27) Baskin, I. I.; Bagatur'yants, A. A.; Gromov, S. P.; Alfimov, M. V. *Dokl. Akad. Nauk* **1994**, *335*, 313−316; *Dokl. Phys. Chem. (Engl. Transl.)* **1994**, *335*, 55−57.
(28) Freidzon, A. Ya.; Baskin, I. I.; Bagatur'yants, A. A.; Gromov, S. P.; Alfimov, M. V. *Izv. Akad. Nauk, Ser. Khim.* **1998**, 2185−2191; *Russ. Chem. Bull. (Engl. Transl.)* **1998**, *47*, 2117−2123.

SCHEME 3

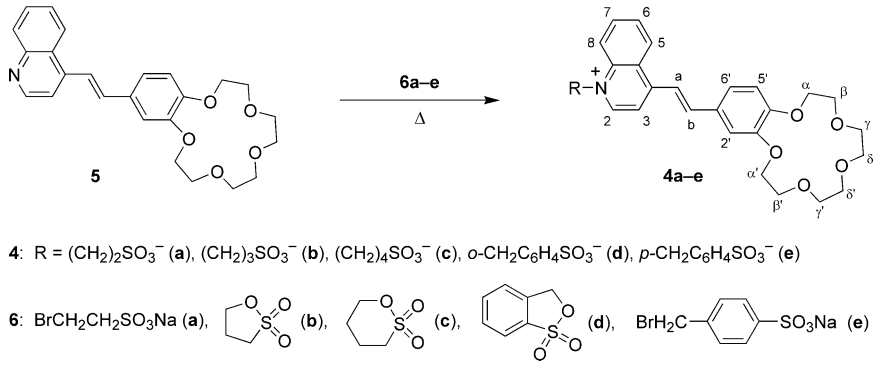

SCHEME 4

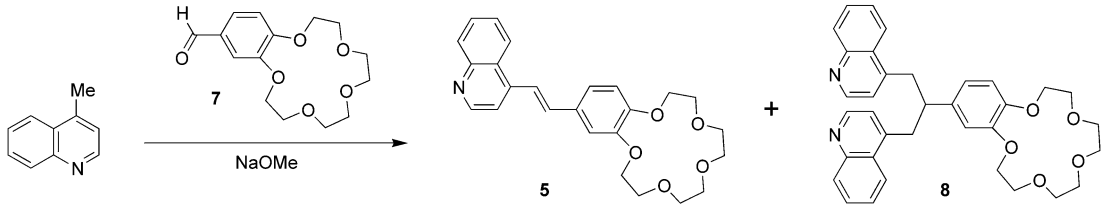

SCHEME 5

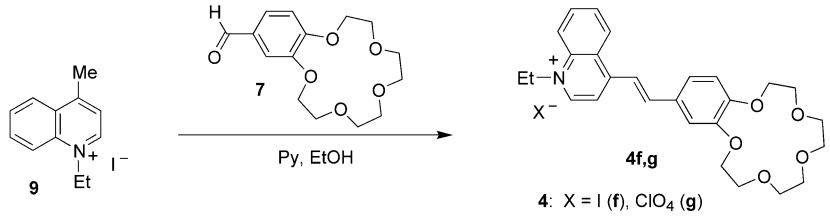

deriving from charge redistribution within the dye induced by Mg^{2+} coordination to the crown ether moiety[7,9,13] (Scheme 6).

Irradiation of (*E*)-**4a**−**e** in air-equilibrated MeCN with visible light led to reversible $E \rightarrow Z$ isomerization. The *Z*-isomers of dyes **4a**−**e** are stable in the dark at ambient temperature, and the reverse $Z \rightarrow E$ isomerization occurred photochemically. For all of the dyes, the *E*-isomer predominated in the photostationary $E \leftrightarrow Z$ equilibria attained on irradiation with 365, 405, or 436 nm light. Quantum yield measurements for **4e** (Table 2) demonstrate that this effect derives from the very low efficiency of the forward geometric isomerization ($\varphi_{E\rightarrow Z} = 0.009$ vs $\varphi_{Z\rightarrow E} = 0.49$).

For donor−acceptor-substituted stilbenes and styryl dyes, in which strong internal charge transfer along the ethylene chain occurs upon excitation, there exist several possible routes of nonradiative decay of the excitation energy.[29] These include rotation around the central C=C bond, resulting in geometric isomerization, or rotation around one or two single bonds in the C−C=C−C fragment, leading to a twisted intramolecular charge-

TABLE 1. Absorption Maximum[a] for Dyes (*E*)-4a−e in MeCN in the Absence and in the Presence of $Mg(ClO_4)_2$[b]

	$\lambda_{max} \pm 1$/nm		
	without cationic complexant	complexed to $Mg(ClO_4)_2$	$\Delta\lambda$[c]/nm
(*E*)-**4a**	440	403	−37
(*E*)-**4b**	440	400	−40
(*E*)-**4c**	440	400	−40
(*E*)-**4d**	445	408	−37
(*E*)-**4e**	449	407	−42

[a] Only the longest wavelength absorption is tabulated here. [b] 1.2×10^{-5} M dye, 1.2×10^{-4} M $Mg(ClO_4)_2$. [c] $\Delta\lambda$ is the $Mg(ClO_4)_2$-induced shift of λ_{max}.

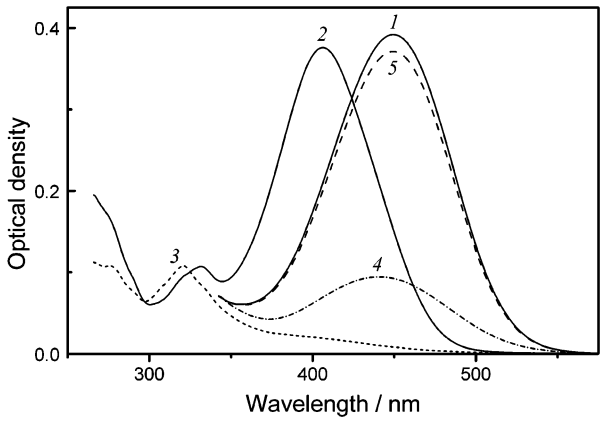

FIGURE 1. Absorption spectra of (*E*)-**4e** (1.2×10^{-5} M, 1 cm cell) in MeCN in the absence of added metal salt (1) and in the presence of 2×10^{-4} M $Mg(ClO_4)_2$ (2). Curves 3−5 are the spectra of the $Mg(ClO_4)_2$-containing solution after irradiation with 436 nm light, assigned as (*Z*)-**4e**·Mg^{2+} (3), after subsequent addition of H_2O (5% v/v), assigned as (*Z*)-**4e** (4), and after subsequent irradiation with 436 nm light up to the photostationary state, assigned as (*E*)/(*Z*)-**4e** (5). Spectra 4 and 5 are corrected for dilution of the starting solution with H_2O.

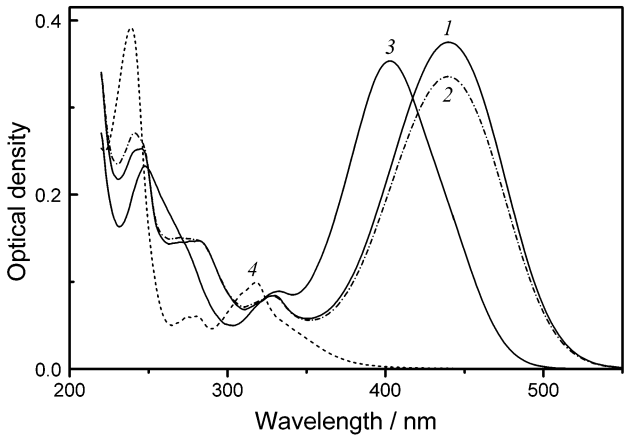

FIGURE 2. Absorption spectra of (*E*)-**4a** (1.2×10^{-5} M, 1 cm cell) in MeCN in the absence of added metal salt (1) and in the presence of 1.2×10^{-4} M $Mg(ClO_4)_2$ (2). Curve 3 is the spectrum of the metal-free solution in the photostationary state attained upon irradiation with 436 nm light. Curve 4 is the spectrum of the $Mg(ClO_4)_2$-containing solution after photolysis with 405 nm light (cycloadduct **10a**).

SCHEME 6

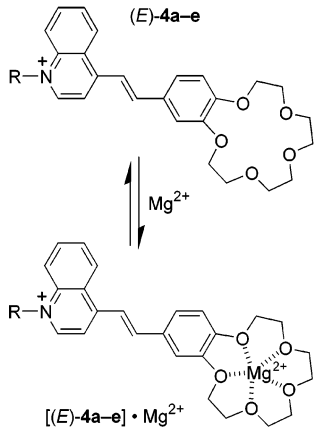

TABLE 2. Quantum Yields of the Reversible PCA and *E* → *Z* Photoisomerization for Dyes 4a−d[a]

	$\varphi_{E\rightarrow Z}$	$\varphi_{Z\rightarrow E}$	φ_{PCA}[b]	$\varphi_{retro-PCA}$[c]
4a + $Mg(ClO_4)_2$	0.08	–	0.20	0.019
4b + $Mg(ClO_4)_2$	0.10	–	0.13	0.010
4c + $Mg(ClO_4)_2$	0.14	–	0.073	0.010
4d + $Mg(ClO_4)_2$	–	–	0.024	0.011
4e + $Mg(ClO_4)_2$[d]	0.20	0.42	–	–
4e	0.009	0.49	–	–

[a] MeCN, 1.2×10^{-5} M dye, 1.2×10^{-4} M $Mg(ClO_4)_2$, ambient temperature. [b] The quantum yields are estimated to within about 20%. The quantum yields of PCA and *E* → *Z* photoisomerizations are measured upon irradiation with 436 nm light. [c] Quantum yields of retro-PCA are measured upon irradiation with 313 nm light. [d] The quantum yield of *Z* → *E*-photoisomerization for **4e** in the presence of $Mg(ClO_4)_2$ is measured upon irradiation with 313 nm light.

transfer (TICT) excited state, which returns to the ground state without geometric isomerization. The forward *E* → *Z* photoisomerization of **4a**−**e** is probably suppressed by a competing process involving the TICT excited state. This assumption is supported by the fact that the complexation of (*E*)-**4e** with Mg^{2+} results in a significant increase in the quantum yield of *E* → *Z* isomerization (Table 2). The crowned Mg^{2+} likely destabilizes the TICT excited state of (*E*)-**4e**, because the metal ion hinders charge transfer from the electron-donating benzocrown group to the electron-accepting quinoline residue.

Although the *Z* → *E* isomerization for the metal-complexed form of **4e** is more efficient than the forward reaction ($\varphi_{Z\rightarrow E} = 0.42$ vs $\varphi_{E\rightarrow Z} = 0.20$), the *Z*-isomer content in the photostationary equilibrium, attained on exposure to 436 nm light, could be increased dramatically (up to 97%) by controlling the incident wavelength. This is because the complexed form of (*Z*)-**4e** [(*Z*)-**4e**]·Mg^{2+} exhibits virtually no absorption in the visible region, so that only the *E*-isomer is converted, shifting the equilibrium strongly toward the *Z*-isomer (Figure 1, curve 3), and its absorptivity at 436 nm is negligible in comparison with that of the complexed form of (*E*)-**4e**. This spectroscopic feature is very likely to arise from the intramolecular coordination of the sulfonate anion to the Mg^{2+} ion associated with the crown ether moiety of (*Z*)-**4e** (Scheme 7).

In the anion-capped complex [(*Z*)-**4e**]·Mg^{2+}, the dye most likely adopts a twisted conformation with disrupted π-conjugation, the feature responsible for the long-wavelength absorption intensity.[30] Similar spectroscopic effects were reported previously for the anion-capped complexes of the *Z*-isomers of dyes **1a**−**d**.[22,25]

Upon the addition of H_2O (5%, v/v), the photochemically obtained complex [(*Z*)-**4e**]·Mg^{2+} was dissociated, releasing Mg^{2+}, which was then strongly solvated by water. The uncomplexed form (*Z*)-**4e** exhibits an absorption band at 441 nm (Figure 1), and subsequent irradiation of this solution with 436 nm light led to a photostationary equilibrium between the *E*- and *Z*-isomers of the metal ion-free form of **4e**. The absorption spectrum of the resulting mixture (Figure 1, curve 5) shows strong similarities to that of the photostationary mixture obtained directly upon irradiation of a metal-free solution of **4e** (the *Z*-isomer:*E*-isomer ratio for this mixture is 1:14).

When using the same four-stage procedure on solutions of (*E*)-**4a**−**d**, i.e., (i) addition of $Mg(ClO_4)_2$ in acetonitrile, (ii) irradiation at 436 nm, (iii) addition of H_2O, and (iv) irradiation at 436 nm, we observed incomplete recovery of the initial dye. This indicates that the metal-complexed forms of (*E*)-**4a**−**d** undergo another photoreaction parallel to *E* → *Z* isomerization that leads ultimately to dye consumption. Virtually complete consumption of **4a**−**d** in $Mg(ClO_4)_2$-containing acetonitrile solutions was reached upon extended photolysis with 405 nm light. The absorption spectrum of the photolyzate obtained from dye **4a** is shown in Figure 2.

The ^1H NMR spectra of the photolyzates (Experimental Section) were analyzed using COSY and NOESY spectroscopy. This analysis showed that the complexed forms of (*E*)-**4a**−**d** undergo stereospecific PCA, i.e., photocyclodimerization, to afford a single cyclobutane stereoisomer in each case (**10a**−**d**, respectively, Scheme 8). The photolyzates contained no other detectable components;

(29) Strehmel, B.; Rettig, W. *J. Biomed. Opt.* **1996**, *1*, 98−109.

(30) Baskin, I. I.; Burshtein, K. Ya; Bagatur'yants, A. A.; Gromov, S. P.; Alfimov, M. V. *J. Mol. Struct.* **1992**, *274*, 93−104.

SCHEME 7

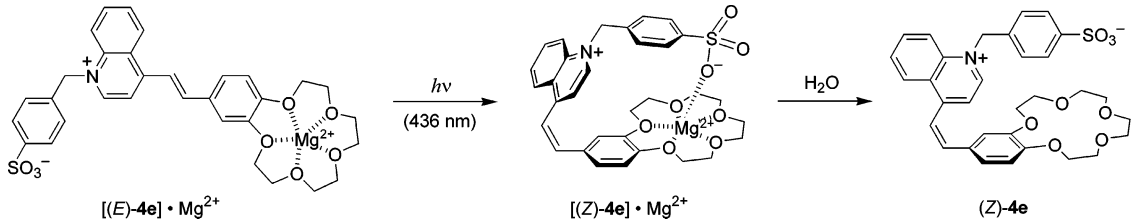

SCHEME 8

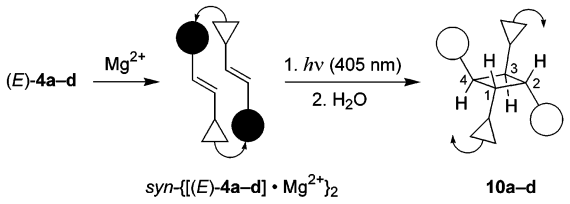

i.e., the cyclobutanes **10a**−**d** are obtained from the corresponding dyes in almost quantitative yields (>95%).

The ^{1}H NMR spectra of the cyclobutane protons in compounds **10a**−**d** (illustrated in Figure 3 for **10b**) can be described by an AA′BB′ spin system with the following set of vicinal coupling constants: $^3J_{H-1,H-2} = {}^3J_{H-3,H-4} =$ 10.4 Hz and $^3J_{H-1,H-4} = {}^3J_{H-2,H-3} =$ 7.7 Hz for **10a**, $^3J_{H-1,H-2} = {}^3J_{H-3,H-4} =$ 10.29 Hz and $^3J_{H-1,H-4} = {}^3J_{H-2,H-3} =$ 7.61 Hz for **10b**, $^3J_{H-1,H-2} = {}^3J_{H-3,H-4} =$ 10.1 Hz and $^3J_{H-1,H-4} = {}^3J_{H-2,H-3} =$ 7.3 Hz for **10c**, $^3J_{H-1,H-2} = {}^3J_{H-3,H-4} =$ 10.6 Hz and $^3J_{H-1,H-4} = {}^3J_{H-2,H-3} =$ 7.6 Hz for **10d**. These values for vicinal coupling constants correlate well with reported values for 1,2,3,4-tetrasubstituted cyclobutane derivatives.[31]

Examination of the spectrophotometric data on the kinetics of the PCA reaction for **4a**−**d** revealed that the *Z*-isomers of **4a**−**d** are not involved in this photoreaction. The structure of **10a**−**d** suggests that these cycloadducts result from concerted *syn*-head-to-tail cycloaddition of *E*-isomer molecules. Intermolecular [2+2]-PCA reactions of olefins are controlled by diffusion and are normally inefficient and not stereospecific in homogeneous solutions, especially at low concentrations of reactants.[14,32] In the presence of Mg^{2+} or Ca^{2+}, however, stereospecific PCA of crown-containing benzothiazolium styryl dyes **1a**−**d**, even in dilute MeCN, has been reported (Scheme 2).[25,26] The *E*-isomers of **1a**−**d** form 2:2 complexes with Mg^{2+} or Ca^{2+}, which provide favorable conditions for [2+2]-PCA. The *anti*-head-to-tail alignment of the two dye molecules in these metalated complexes is responsible for the selective formation of the corresponding cycloadduct in the PCA reaction.[25]

To interpret the $Mg(ClO_4)_2$-induced stereospecific PCA of **4a**−**d** in dilute MeCN, we assume that the *E*-isomers of these dyes form 2:2 complexes with Mg^{2+}, so that the two dyes are arranged *syn*-head-to-tail (Scheme 8). With **4a**−**d**, the quantum yields of PCA remained almost unchanged as the dye concentration increased from 1.2×10^{-5} to 1.2×10^{-4} M at a fixed 1×10^{-4} M excess of $Mg(ClO_4)_2$ over the dye. These data point to unimolecular kinetics for cyclobutane formation by the PCA reaction. In addition, these data show a dimerization equilibrium constant for the complexes [(*E*)-**4a**−**d**]·Mg^{2+} in MeCN significantly larger than 10^5 M^{-1}.

We suppose that the *Z*-isomers of **4a**−**d**, like that of **4e**, are able to form anion-capped 1:1 complexes with Mg^{2+}. Hence, the existence of dimeric complexes of (*Z*)-**4a**−**d** with Mg^{2+} is unlikely in dilute solutions. This conclusion is in agreement with the fact that the Mg^{2+} complexes of (*Z*)-**4a**−**d** do not undergo photocycloaddition.

The quantum yields of photoreactions of **4a**−**d** in $Mg(ClO_4)_2$-containing MeCN are listed in Table 2. The structure of the *N*-substituent bearing the terminal SO_3^- group has a significant effect on the PCA efficiency, but does not influence the stereospecificity of this reaction. The *N*-substituent brings the C=C bonds to within bonding distances in the dimeric complex. The structure of the dimeric complex affects the PCA efficiency. The quantum yield of PCA decreases and the quantum yield of the competing $E \rightarrow Z$ isomerization increases as the length of the sulfonatoalkyl spacer increases in **4a**−**c**, Table 2. The more rigid *o*-sulfonatobenzyl spacer in **4d** produces a significant decrease in the quantum yield of PCA, and this reaction becomes even more inefficient with the *p*-sulfonatobenzyl spacer.

The cyclobutanes **10a**−**d** are stable in the dark but can undergo the reverse photoreaction, i.e., retro-PCA, on exposure to UV light. In $Mg(ClO_4)_2$-containing solutions, the retro-PCA for **10a**−**d** occurs with a quantum yield ranging from 0.02 to 0.01.

In metal-free solutions, i.e., in those with no supramolecular organization, dyes **4a**−**d** do not undergo PCA even at higher concentrations ([dye] $\approx 10^{-3}$ M). Probably this contrasting reactivity relates to the absence of the oriented complex at equilibrium, to the high degree of conjugation involving the double C=C bond in the dye molecules, and to the short lifetime of the excited states of these dyes.

Theoretical Studies of Dimeric Metal Complexes and PCA. Earlier, we demonstrated the utility of molecular mechanics calculations to explain the relative

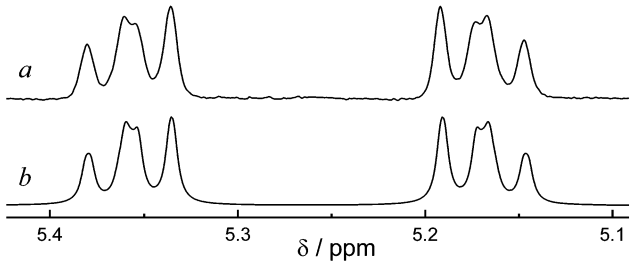

FIGURE 3. Experimental (a) and computer-simulated (b) ^{1}H NMR spectra of the cyclobutane protons of **10b** (Bruker AMX-400, 400.13 MHz, D_2O, 321 K).

(31) Danati, D.; Fiorenza, M.; Fautoni, P. S. *J. Heterocycl. Chem.* **1979**, *16*, 253−256.

(32) Klessinger, M.; Michl, J. *Excited States and Photochemistry of Organic Molecules*; VCH: New York, 1995.

SCHEME 9

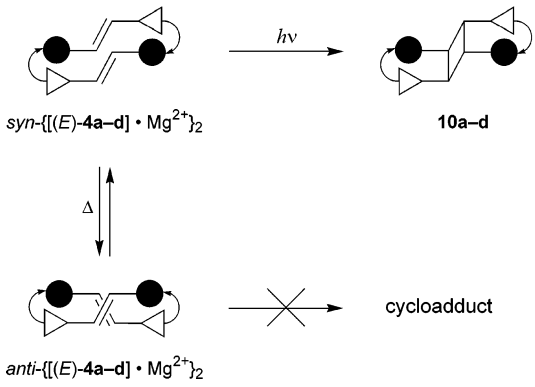

SCHEME 10

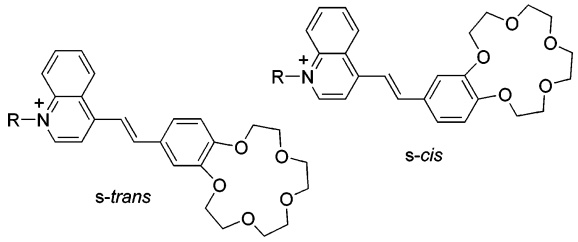

photoefficiency and stereoselectivity of PCA in dimeric complexes of various crown-containing styryl dyes.[27,28] As reported, the following results were obtained: (i) for closely related dyes, the quantum yield of PCA correlates well with the heat of the dimer-to-cycloadduct photoreaction; (ii) in most cases, the calculated energies of *syn*- and *anti*-conformers of the dimeric metal complexes are very close; (iii) for **4a**−**e**, the *anti*-conformers have a skewed relative orientation (Scheme 9) of the two C═C bonds, which is unfavorable for the PCA reaction.

Here we report a more comprehensive theoretical study of PCA in dimeric complexes {[(*E*)-**4a**−**e**]·Mg^{2+}}$_2$, including simulation of numerous conformations of these complexes, analysis of molecular dynamics trajectories, and semiempirical quantum chemical calculations. Molecular mechanics and molecular dynamics computations were done using the MMX force field implemented in the PCMODEL program.[33] This force field has been adapted for organic molecules containing conjugated double bonds and/or coordination with metal ions. Semiempirical quantum chemical calculations were performed using the PM3 method.

To simplify the molecular mechanics computations, only those hydrogen atoms attached to the central C═C bond of the dye were considered explicitly, while all the other hydrogen atoms were included in a united atom approach.[27,28] The initial geometry of the dye assumed two single bond rotational isomers, *s-trans* and *s-cis*, as depicted in Scheme 10.

Rotational isomerism around the single bond in the Het−C═C fragment was not considered because the alternative isomer is unlikely because of repulsion between the H-5 quinolinium and the H-b olefinic hydrogen atoms. For each dimeric metal complex, six principal conformations were constructed, differing from each other either in the combination of the dye *s*-rotamers (*s-trans*,*s-trans*, *s-cis*,*s-cis*, or *s-trans*,*s-cis*) or in the relative orientation (*syn* or *anti*) of the two C−C═C−C fragments. The geometry of each conformer was then optimized using the conformation search method reported previously.[27,28] The obtained structures (as shown in Figure 4 for the *syn*-(*s-trans*,*s-trans*)-conformer of {[(*E*)-**4a**]·Mg^{2+}}$_2$) were further optimized with the PM3 quantum chemical method. The same approach was used to simulate the cycloadducts corresponding to the *syn*-conformers of the dimeric complexes.

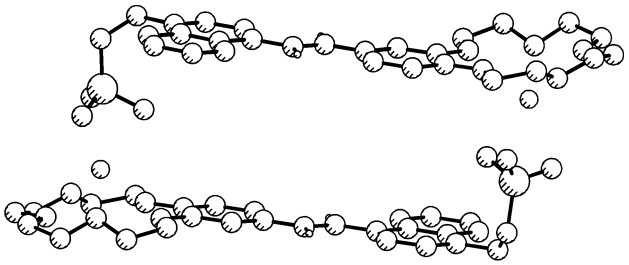

FIGURE 4. MMX-optimized geometry of the *syn*-(*s-trans*,*s-trans*)-conformer of dimeric complex {[(*E*)-**4a**]·Mg^{2+}}$_2$.

Heats of formation, energy differences, and the distance between π,π closest approach obtained from the MMX and PM3 calculations for the three possible *syn*-conformers of the dimeric complexes {[(*E*)-**4a**−**e**]·Mg^{2+}}$_2$ are given in Table 3.

In most cases, the difference in the heat of formation between the *syn*-conformers of a particular dimeric complex is very small. In addition, the calculated H_f values for the most stable *syn*-conformers proved to be very close to those for the corresponding *anti*-conformers. Although in some cases there is a disagreement between the MMX and PM3 predictions about the most stable conformer, both methods predict coexistence of multiple conformers of the dimeric complexes.

The distance between two reacting C═C bonds (R) and the steric hindrance encountered in the approach of these bonds to within cyclobutane bonding distance are important factors influencing the quantum yield of PCA in the dimeric complexes. For closely related dyes, the second factor should correlate with the energetics of the PCA dimerization. A comparison of the experimental data on the PCA efficiency (Table 2) with the calculated parameters R and ΔE for the most stable *syn*-conformers (Table 3), however, shows that neither of these parameters correlates separately with the PCA quantum yield. To interpret the experimental data, both parameters have to be taken into account.

For the dyes **4a**−**c** with a flexible sulfonatoalkyl group, the PCA quantum yield increases as the distance between the C═C bonds in the dimeric complex decreases. On the other hand, the PCA quantum yield for **4d** is considerably lower than that for **4c**, despite the shorter distance between the C═C bonds in {[(*E*)-**4d**]·Mg^{2+}}$_2$. This is attributable to stronger steric hindrance to the cycloaddition in this complex, resulting from the relative rigidity of the *o*-sulfonatobenzyl linker. Such steric hindrance causes PCA to be energetically less favorable for **4d** than for **4c**.

According to our calculations, the dimeric complex {[(*E*)-**4e**]·Mg^{2+}}$_2$ is characterized by a relatively long distance between the C═C bonds and by very strong

(33) PCMODEL, Serena Software, Bloomington, IN.

TABLE 3. Data from MMX and PM3 Calculations for Three Possible *syn*-Conformers of Dimeric Complexes (*E*)-4a−e with Mg^{2+} [a]

	syn-{[(*E*)-**4a**]·Mg^{2+}}$_2$			*syn*-{[(*E*)-**4b**]·Mg^{2+}}$_2$			*syn*-{[(*E*)-**4c**]·Mg^{2+}}$_2$			*syn*-{[(*E*)-**4d**]·Mg^{2+}}$_2$			*syn*-{[(*E*)-**4e**]·Mg^{2+}}$_2$		
param (method)	*s-trans*, *s-trans*	*s-cis*, *s-trans*	*s-cis*, *s-cis*	*s-trans*, *s-trans*	*s-cis*, *s-trans*	*s-cis*, *s-cis*	*s-trans*, *s-trans*	*s-cis*, *s-trans*	*s-cis*, *s-cis*	*s-trans*, *s-trans*	*s-cis*, *s-trans*	*s-cis*, *s-cis*	*s-trans*, *s-trans*	*s-cis*, *s-trans*	*s-cis*, *s-cis*
H_f (MMX)	87.6	88.8	89.6	92.1	92.5	93.7	88.3	87.0	88.1	158.0	158.5	162.4	153.8	156.4	153.0
ΔE (MMX)	−8.6	−10.4	−9.9	−14.0	−11.0	−7.8	−13.2	−7.4	−6.2	−4.2	−1.7	−5.5	+27.2	+25.1	+ 30
R (MMX)	6.5	6.6	6.4	8.0	6.8	7.6	8.4	8.7	8.9	7.3	6.6	6.9	11.1	10.8	10.3
H_f (PM3)	358.7	317.5	360.0	329.6	322.7	334.1	307.2	308.8	310.9	403.6	385.9	403.3	385.0	384.9	382.8
ΔE (PM3)	+14.7	+41.9	−6.5	+1.0	−4.2	−13.6	−16.7	−1.7	0.0	+19.6	+54.0	−17.6	−31.5	−32.3	−37.1
R (PM3)	7.9	8.7	7.8	9.8	9.3	9.7	9.9	9.6	9.9	8.3	8.4	8.5	11.6	11.5	11.2

[a] H_f is the heat of formation (kcal mol^{-1}) of the dimeric complex, ΔE is the difference in energy (kcal mol^{-1}) between the cycloadduct and the initial dimeric complex, and *R* is the mean distance (Å) between the nearest atoms of the two C=C bonds in the dimeric complex.

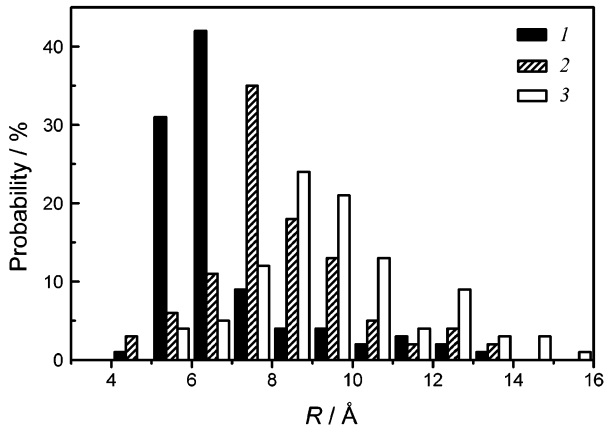

FIGURE 5. Molecular dynamics distributions of the mean distance (*R*) between the nearest atoms of the two C=C bonds for the most stable *syn*-conformers of the {[(*E*)-**4a**]·Mg^{2+}}$_2$ (*1*), {[(*E*)-**4b**]·Mg^{2+}}$_2$ (*2*), and {[(*E*)-**4c**]·Mg^{2+}}$_2$ (*3*) dimeric complexes.

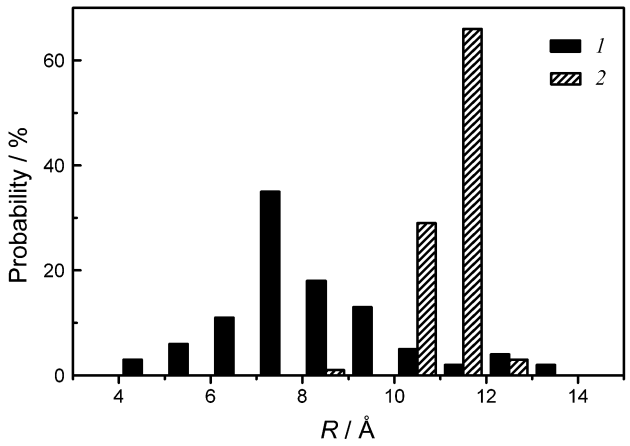

FIGURE 6. Molecular dynamics distributions of the mean distance (*R*) between the nearest atoms of the two C=C bonds for the most stable *syn*-conformer (*1*) and *anti*-conformer (*2*) of the {[(*E*)-**4b**]·Mg^{2+}}$_2$ dimeric complex.

steric hindrance to the approach to bonding distance of these bonds; thus, this complex cannot undergo PCA.

For all dimeric complexes studied, the distance between the C=C bonds in the geometrically optimized complex considerably exceeds the maximum distance at which PCA bond formation can occur (about 4 Å). To rationalize this fact, we carried out molecular dynamics simulations for the most stable *syn*-conformers of complexes {[(*E*)-**4a**−**c**]·Mg^{2+}}$_2$ at 300 K. During each 10 ps molecular dynamics run, 100 conformations were collected in 0.1 ps increments so that the distribution of the parameter *R* within this set of conformations obtained could be calculated. The histograms in Figure 5 represent the calculated distributions for complexes {[(*E*)-**4a**−**c**]·Mg^{2+}}$_2$. These data demonstrate that the dimeric complexes are sufficiently flexible to allow the double bonds to approach to a distance required for PCA over a 10 ps molecular dynamics run.

As noted above, our calculations predict the coexistence of *syn*- and *anti*-conformers of the dimeric complexes {[(*E*)-**4a**−**e**]·Mg^{2+}}$_2$. The selective formation of the *syn*-head-to-tail photocycloadducts under these conditions can be explained by the fact that the *anti*-conformers have a skewed relative orientation of the two C=C bonds, which is unfavorable for PCA.[27,28] The stereospecificity of PCA was rationalized in a 10 ps molecular dynamics run for the most stable *anti*-conformer of the {[(*E*)-**4b**]·Mg^{2+}}$_2$ dimeric complex. The histograms in Figure 6 make it possible to compare the distributions of the parameter *R* for the *anti*- and *syn*-conformers of this complex. Thus, the double bonds in the *anti*-conformer are remote from each other and cannot approach each other to a range within the distance required for PCA over the time constraints of a molecular dynamics run.

NMR Study of Dimeric Metal Complexes. A ^1H NMR study of the complexation of dyes (*E*)-**4b** and (*E*)-**4g** with $Mg(ClO_4)_2$ in MeCN-d_3 confirmed the theoretical predictions of various conformers coexisting in the dimeric complexes. The proton magnetic resonance chemical shifts for dyes (*E*)-**4b** and (*E*)-**4g** and for their metal-complexed forms are listed in Table 4. Figure 7 shows the effect of complexation with Mg^{2+} on the ^1H NMR spectrum of (*E*)-**4b**.

Dye (*E*)-**4g** is an almost complete analogue of (*E*)-**4b**; however, it does not contain a sulfonate group and, hence, is unable to form dimeric complexes. In the absence of added metal salt, dyes (*E*)-**4b** and (*E*)-**4g** show almost equal proton chemical shifts. Upon the addition of $Mg(ClO_4)_2$, all proton signals of (*E*)-**4g** shift downfield, pointing to complex formation.[34] The greatest shifts are observed for the crown ether protons located most closely to the complexed Mg^{2+}. As the distance between the observed proton and the complexed metal cation increases, the downfield shift diminishes. Nevertheless, noticeable changes in the chemical shifts are observed

(34) Fedorov, L. A.; Ermakov, A. N. *Spektroskopiya YaMR v Neorganicheskom Analize* (*NMR Spectroscopy in Inorganic Analysis*); Nauka: Moscow, 1989; Chapters 2 and 3 (in Russian).

TABLE 4. ^{1}H NMR Chemical Shifts for Dyes (*E*)-**4g** and (*E*)-**4b** and for Their Complexes with $Mg(ClO_4)_2$ in MeCN-d_3 at Ambient Temperature[a]

	δ/ppm										
	H(C-2′)	H(C-5′)	H(C-6′)	H(C-a)	H(C-b)	H(C-2)	H(C-3)	H(C-5)	H(C-6)	H(C-7)	H(C-8)
(*E*)-**4g**	7.47	7.00	7.40	7.95	7.95	8.97	8.23	8.85	7.97	8.20	8.30
[(*E*)-**4g**]·Mg^{2+}	7.8	7.35	7.65	8.20	8.00	9.00	8.3	8.95	8.1	8.25	8.40
Δδ	0.33	0.35	0.25	0.25	0.05	0.03	0.07	0.1	0.13	0.05	0.10
(*E*)-**4b**[b]	7.44	7.01	7.36	7.91	7.87	8.95	8.16	8.79	7.96	8.19	8.41
{[(*E*)-**4b**]·Mg^{2+}}$_2$ (F_1)	7.15	7.18	7.00	7.33	7.10	8.7	7.88	8.63	8.13	8.30	8.30
Δδ	−0.29	0.17	−0.36	−0.58	−0.77	−0.25	−0.28	−0.16	0.17	0.11	−0.11
{[(*E*)-**4b**]·Mg^{2+}}$_2$ (F_2)	7.35	7.23	6.8	7.20	6.95	8.85	7.90	8.70	8.13	8.15	7.95
Dd	−0.09	0.22	−0.56	−0.71	−0.92	−0.1	−0.26	−0.09	0.17	−0.04	−0.46

	δ/ppm								
	NCH_2	CH_3	CH_2	$CH_2SO_3^-$	H(C-α)	H(C-α′)	H(C-β,β′)	H(C-γ,γ′)	H(C-δ,δ′)
(*E*)-**4g**	4.9	1.65			4.2	4.25	3.85	3.7	3.7
[(*E*)-**4g**]·Mg^{2+}	4.95	1.7			4.65	4.7	3.9−4.3	3.9−4.3	3.9−4.3
Δδ	0.05	0.05			0.45	0.45	0.05−0.45	0.2−0.6	0.2−0.6
(*E*)-**4b**[b]	5.04		2.45	2.94	4.17	4.23	3.8−3.9	3.6−3.7	3.6−3.7
{[(*E*)-**4b**]·Mg^{2+}}$_2$ (F_1)	4.3−4.6		1.9	3.0	4.5−4.7	4.5−4.7	4.3	4.1	4.5−3.9
Dd	−(0.44−0.74)		−0.55	0.06	0.33−0.53	0.27−0.47	0.4−0.5	0.4−0.5	0.2−0.9
{[(*E*)-**4b**]·Mg^{2+}}$_2$ (F_2)	4.3−4.6		1.9	3.0	4.5−4.7	4.5−4.7	4.15	4.0	4.5−3.9
Δδ	−(0.44−0.74)		−0.55	0.06	0.33−0.53	0.27−0.47	0.25−0.35	0.3−0.4	0.2−0.9

[a] Protons are numbered according to Scheme 3; δ is the proton chemical shift and Δδ = δ(complex) − δ(free dye). [b] To measure the δ values for (*E*)-**4b**, decomplexation with D_2O (5%, v/v) was used.

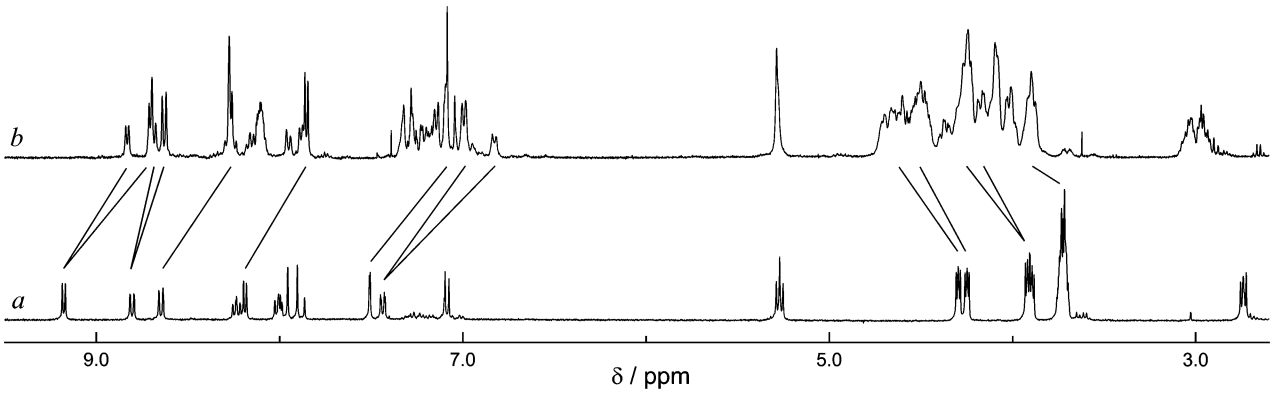

FIGURE 7. ^{1}H NMR spectra of dye (*E*)-**4b** (*a*) and its Mg^{2+}-complexed forms (*b*) in MeCN-d_3 at 295 K. Straight lines show the changes in the proton chemical shifts induced by complexation.

even for the rather remote protons of the C═C bond, a phenomenon which is due to the efficient electron-withdrawing effect of Mg^{2+} along the conjugated chain of the chromophore.

The ^{1}H NMR spectrum of the Mg^{2+}-complexed form of dye (*E*)-**4b** consists of two groups of signals corresponding to two species, F_1 and F_2, present in a 10:3 ratio. Analysis of the 2D NOESY spectrum (Supporting Information, Figure S1) showed that these species are in dynamic equilibrium. At room temperature, the exchange time is fairly long on the NMR time scale, which allows the resonance lines for these species to be observed separately. The coalescence point for F_1 and F_2 is at about 70 °C, which corresponds to an activation barrier to the exchange reaction of 16−17 kcal mol^{-1}.

For both F_1 and F_2, most of the signals for aromatic and olefinic protons are shifted upfield from the corresponding signals for the uncomplexed form of (*E*)-**4b**. Thus, neither F_1 nor F_2 can be identified as a 1:1 complex. The observed upfield shifts are consistent with the formation of the dimeric complexes {[(*E*)-**4b**]·Mg^{2+}}$_2$ with a head-to-tail alignment of the dyes and a parallel stacking of the aromatic rings. Thus, the benzene moiety of the benzocrown fragment of one dye molecule falls into the shielding cone of the heteroaromatic fragment of the second molecule and vice versa.

In principle, the two species F_1 and F_2 could be rationalized by the formation of a single conformer of the dimeric complex that contains both *s-trans*- and *s-cis*-rotamers of the dye, for example, *syn*-(*s-trans*,*s-cis*)-{[(*E*)-**4b**]·Mg^{2+}}$_2$. However, this interpretation is at variance with the fact that species F_1 and F_2 are present in unequal amounts (10:3). Thus, dimeric complexes with an *s-trans*,*s-cis*-combination of rotamers are not formed, allowing contribution of only four possible conformers: *syn*-(*s-trans*,*s-trans*), *syn*-(*s-cis*,*s-cis*), *anti*-(*s-trans*,*s-trans*), and *anti*-(*s-cis*,*s-cis*). The presence of two species, F_1 and F_2, is, apparently, due to the coexistence of two of these four conformers of {[(*E*)-**4b**]·Mg^{2+}}$_2$. The significant difference between the NMR spectra of F_1 and F_2 indicates that the two coexisting conformers of this complex are characterized by different relative orientations of the C—C═C—C fragments (*syn* and *anti*). Unfortunately, we were unable to assign unambiguously species F_1 and F_2,

given that NOE measurements do not allow determination of the specific *s*-rotamer in the dimeric complex, because the proton signals for the benzocrown ether and the C=C bond overlap significantly.

Summary

Crown-containing styryl dyes of a series of substituted quinolines bearing a sulfonatoalkyl or sulfonatobenzyl group can act as chromoionophores and as photoswitchable ionophores, because of their ability to undergo reversible $E \rightarrow Z$ photoisomerization, leading to anion-capped 1:1 metal complexes. The *E*-isomers of these dyes form highly stable dimeric complexes with Mg^{2+}. When associated in such a complex, stereoselective photoinduced [2+2]-cycloaddition between the substrates is highly efficient. Systematic modification of the *N*-substituent containing the terminal SO_3^- group makes it possible to specify the direction of photochemical conversion of the crown-containing styryl dye and to influence the quantum yields of the two concurrent photoreactions. The dyes studied are of interest as synthons for stereospecific photochemical synthesis of a series of novel host molecules, i.e., bis-crown-containing cyclobutanes.

Experimental Section

Materials. 4-Methylquinoline, sodium 2-bromoethanesulfonate (**6a**), 1,3-propane sultone (**6b**), and 1,4-butane sultone (**6c**) were commercially available. 4′-Formylbenzo-15-crown-5 ether (**7**),[35] γ-sultone (**6d**),[36] sodium 4-bromomethylbenzenesulfonate (**6e**),[37] and 1-ethyl-4-methylquinolinium iodide[38] (**9**) were synthesized according to known procedures. Anhydrous $Mg(ClO_4)_2$ was used as received. Spectroscopic grade MeCN was distilled over CaH_2 to remove traces of water. Solutions of dyes **4a**−**e** were prepared and manipulated under red light.

Reaction of 4-Methylquinoline with 4′-Formylbenzo-15-crown-5 Ether (7). A mixture of 4-methylquinoline (0.13 mL, 1.0 mmol), compound **7** (0.44 g, 1.5 mmol), and NaOMe (0.054 g, 1.0 mmol) was dissolved in anhyd DMSO and kept for 72 h at rt. Distilled water was then added, and the mixture was extracted with benzene. The benzene extract was dried and evaporated to a give viscous yellow oil that was loaded onto an aluminum oxide column. The products were eluted with a benzene/ethyl acetate mixture to give compounds **5** (0.051 g, 12%) and **8** (0.35 g, 63%). When the same reaction was carried out in the presence of $NaClO_4$ (2 mmol of $NaClO_4$, 1 mmol of 4-methylquinoline, 2 mmol of **7**, and 0.5 mmol of NaOMe), the yields of **5** and **8** were 28% and 2%, respectively.

4-[(*E*)-2-(2,3,5,6,8,9,11,12-Octahydro-1,4,7,10,13-benzopentaoxacyclopentadecin-15-yl)-1-ethenyl]quinoline (5). Mp: 81−84 °C. ^{1}H NMR (DMSO-d_6): δ 3.74 (s, 8 H, γ,γ′,δ,δ′-CH_2O), 3.91 (m, 4 H, β,β′-CH_2O), 4.20 and 4.30 (m, 4 H, α,α′-CH_2O), 7.10 (d, 1 H, H(C-5′) in benzocrown ether, J = 8.3 Hz), 7.39 (d, 1 H, H(C-6′) in benzocrown ether, J = 8.3 Hz), 7.63 (d, 1 H, H(C-a), J = 16.1 Hz), 7.64 (s, 1 H, H(C-2′) in benzocrown ether), 7.76 and 7.89 (2 m, 2 H, H(C-6), H(C-7) in quinoline), 7.92 (d, 1 H, H(C-3) in quinoline, J = 4.7 Hz), 8.07 (d, 1 H, H(C−b), J = 16.1 Hz), 8.13 (d, 1 H in quinoline, J = 8.3 Hz), 8.66 (d, 1 H in quinoline, J = 8.4 Hz), 8.96 (d, 1 H, H(C-2) in quinoline, J = 4.7 Hz). MS: *m/e* (relative intensity) 421 $[M]^+$ (100), 290 (79), 289 (74), 288 (51), 263 (42), 323 (32), 217 (28), 216 (29), 204 (49), 109 (39), 108 (26). Anal. Calcd for $C_{25}H_{27}NO_5$: C, 71.24; H, 6.46; N, 3.32. Found: C, 70.97; H, 6.68; N, 3.12.

4-[2-(2,3,5,6,8,9,11,12-Octahydro-1,4,7,10,13-benzopentaoxacyclopentadecin-15-yl)-3-(4-quinolyl)propyl]quinoline (8). Mp: 62−65 °C. ^{1}H NMR ($CDCl_3$): δ 3.39 (m, 3 H, CH_2, CH), 3.54 (m, 2 H, CH_2), 3.77 (m, 8 H, γ,γ′,δ,δ′-H_2O), 3.85 and 3.91 (2 m, 4 H, β,β′-CH_2O), 3.96 and 4.10 (2 m, 4 H, α,α′-CH_2O), 6.51 (s, 1 H, H(C-2′) in benzocrown ether), 6.54 (d, 1 H, H(C-6′) in benzocrown ether, J = 8.2 Hz), 6.71 (d, 1 H, H(C-5′) in benzocrown ether, J = 8.2 Hz), 6.99 (d, 2 H, H(C-3) in quinoline, J = 4.4 Hz), 7.40 (d, 2 H in quinoline), 7.65 (d, 2 H in quinoline, J = 8.1 Hz), 7.69 (m, 2 H in quinoline), 8.12 (d, 2 H in quinoline, J = 8.4 Hz), 8.72 (d, 2 H, H(C-2) in quinoline, J = 4.4 Hz). MS: *m/e* (relative intensity) 564 $[M]^+$ (2), 457 (46), 423 (14), 422 (54), 325 (22), 324 (77), 155 (17), 154 (100), 143 (55), 115 (16), 108 (28). Anal. Calcd for $C_{35}H_{36}N_2O_5$: C, 74.45; H, 6.43; N, 4.96. Found: C, 74.64; H, 6.40; N, 4.88.

Synthesis of 4a−e. The appropriate reactant (i.e., **6a**−**e**, 1 mmol) was heated with 1 mmol of crown-containing 4-styrylquinoline **5** at 120 °C for 3−5 h. The reaction mixture was washed with benzene, and the solid product was recrystallized from MeOH. The yield of the styryl dye was 54% for **4a**, 90% for **4b**, 95% for **4c**, 99% for **4d**, and 71% for **4e**.

2-{4-[(*E*)-2-(2,3,5,6,8,9,11,12-Octahydro-1,4,7,10,13-benzopentaoxacyclopentadecin-15-yl)-1-ethenyl]-1-quinoliniumyl}-1-ethanesulfonate (4a). Mp: 199−205 °C. ^{1}H NMR (DMSO-d_6): δ 3.23 (t, 2 H, $CH_2SO_3^-$), 3.73 (s, 8 H, γ,γ′,δ,δ′-CH_2O), 3.92 (m, 4 H, β,β′-CH_2O), 4.25 and 4.32 (2 m, 4 H, α,α′-CH_2O), 5.28 (t, 2 H, CH_2N), 7.19 (d, 1 H, H(C-5′) in benzocrown ether), 7.56 (d, 1 H, H(C-6′) in benzocrown ether), 7.80 (s, 1 H, H(C-2′) in benzocrown ether), 8.12 and 8.35 (2 m, 2 H, H(C-6), H(C-7) in quinoline), 8.22 and 8.28 (2 d, 2 H, H(C-a), H(C-b), J = 15.5 Hz), 8.48 (d, 1 H, H(C-3) in quinoline), 8.54 (d, 1 H in quinoline), 9.15 (d, 1 H in quinoline), 9.35 (d, 1 H, H(C-2) in quinoline). Anal. Calcd for $C_{27}H_{31}NO_8S\cdot 0.5H_2O$: C, 60.21; H, 5.99; N, 2.60. Found: C, 60.32; H, 5.96; N, 2.54.

3-{4-[(*E*)-2-(2,3,5,6,8,9,11,12-Octahydro-1,4,7,10,13-benzopentaoxacyclopentadecin-15-yl)-1-ethenyl]-1-quinoliniumyl}-1-propanesulfonate (4b). Mp: 258−260 °C. ^{1}H NMR (MeCN-d_3): δ 2.50 (m, 2 H, CH_2), 2.74 (m, 2 H, $CH_2SO_3^-$), 3.72 (m, 8 H, γ,γ′,δ,δ′-CH_2O), 3.91 (m, 4 H, β,β′-CH_2O), 4.25 and 4.31 (2 m, 4 H, α,α′-CH_2O), 5.27 (m, 2 H, CH_2N), 7.08 (d, 1 H, H(C-5′) in benzocrown ether, J = 8.3 Hz), 7.43 (dd, 1 H, H(C-6′) in benzocrown ether, J = 8.3 Hz, J = 2.0 Hz), 7.51 (d, 1 H, H(C-2′) in benzocrown ether, J = 2.0 Hz), 7.88 and 7.96 (2 d, 2 H, H(C-a), H(C-b), J = 15.8 Hz), 8.00 (m, 1 H, H(C-6) in quinoline), 8.19 (d, 1 H, H(C-3) in quinoline, J = 6.6 Hz), 8.23 (m, 1 H, H(C-7) in quinoline), 8.65 (d, 1 H, H(C-8) in quinoline, J = 8.9 Hz), 8.80 (d, 1 H, H(C-5) in quinoline, J = 8.6 Hz), 9.18 (d, 1 H, H(C-2) in quinoline, J = 6.6 Hz). Anal. Calcd for $C_{28}H_{33}NO_8S$: C, 61.86; H, 6.12; N, 2.58. Found: C, 61.43; H, 6.08; N, 2.50.

4-{4-[(*E*)-2-(2,3,5,6,8,9,11,12-Octahydro-1,4,7,10,13-benzopentaoxacyclopentadecin-15-yl)-1-ethenyl]-1-quinoliniumyl}-1-butanesulfonate (4c). Mp: 282−284 °C. ^{1}H NMR (DMSO-d_6): δ 1.70 (m, 2 H, CH_2), 2.06 (m, 2 H, CH_2), 2.54 (m, 2 H, $CH_2SO_3^-$), 3.64 (s, 8 H, γ,γ′,δ,δ′-CH_2O), 3.80 and 3.84 (2 m, 4 H, β,β′-CH_2O), 4.15 and 4.22 (2 m, 4 H, α,α′-CH_2O), 4.98 (m, 2 H, CH_2N), 7.09 (d, 1 H, H(C-5′) in benzocrown ether, J = 8.3 Hz), 7.47 (d, 1 H, H(C-6′) in benzocrown ether, J = 8.3 Hz), 7.70 (s, 1 H, H(C-2′) in benzocrown ether), 8.03 (m, 1 H in quinoline), 8.14 and 8.19 (2 d, 2 H, H(C-a), H(C-b), J = J = 15.8 Hz), 8.24 (m, 1 H in quinoline), 8.45 (d, 1 H, H(C-3) in quinoline, J = 6.6 Hz), 8.60 (d, 1 H in quinoline, J = 9.0 Hz), 9.06 (d, 1 H in quinoline, J = 8.6 Hz), 9.35 (d, 1 H, H(C-2) in quinoline, J = 6.6 Hz). Anal. Calcd for $C_{29}H_{35}NO_8S\cdot 1.5H_2O$: C, 59.57; H, 6.55; N, 2.40. Found: C, 59.46; H, 6.12; N, 2.30.

(35) Gromov, S. P.; Fedorova, O. A.; Vedernikov, A. I.; Samoshin, V. V.; Zefirov, N. S.; Alfimov, M. V. *Izv. Akad. Nauk, Ser. Khim.* **1995**, 121−128; *Russ. Chem. Bull. (Engl. Transl.)* **1995**, *44*, 116−123.

(36) Ungaro, R.; Haj, B. E.; Smid, J. *J. Am. Chem. Soc.* **1976**, *98*, 5198−5202.

(37) Hubbuch, A.; Bindewald, R.; Föhles, J.; Kumar, V. *Angew. Chem.* **1980**, *92*, 394−395.

(38) Koral, M.; Bonis, D.; Fusco, A. J.; Dougherty, P.; Leifer, A.; LuValle, J. E. *J. Chem. Eng. Data* **1964**, *9*, 406−407.

2-({4-[(*E*)-2-(2,3,5,6,8,9,11,12-Octahydro-1,4,7,10,13-benzopentaoxacyclopentadecin-15-yl)-1-ethenyl]-1-quinoliniumyl}methyl)-1-benzenesulfonate (4d). Mp: 242−247 °C. ^{1}H NMR (DMSO-d_6): δ 3.66 (m, 8 H, $\gamma,\gamma',\delta,\delta'$-$CH_2O$), 3.84 (m, 4 H, β,β'-CH_2O), 4.20 and 4.26 (2 m, 4 H, α,α'-CH_2O), 6.63 (s, 2 H, CH_2N), 6.74 (d, 1 H, H(C-6″) in sulfonatobenzyl, J = 7.0 Hz), 7.09 (d, 1 H, H(C-5′) in benzocrown ether, J = 8.1 Hz), 7.22 (t, 1 H in sulfonatobenzyl), 7.35 (t, 1 H in sulfonatobenzyl), 7.49 (d, 1 H, H(C-6′) in benzocrown ether, J = 8.1 Hz), 7.63 (s, 1 H, H(C-2′) in benzocrown ether), 7.96 (m, 2 H), 8.09 (m, 3 H), 8.43 (d, 1 H, H(C-3) in quinoline, J = 6.0 Hz), 8.53 (d, 1 H in quinoline, J = 8.5 Hz), 8.95 (d, 1 H in quinoline, J = 8.1 Hz), 9.31 (d, 1 H, H(C-2) in quinoline, J = 6.0 Hz). Anal. Calcd for $C_{32}H_{33}NO_8S\cdot H_2O$: C, 63.04; H, 5.79; N, 2.30. Found: C, 62.88; H, 5.41; N, 2.25.

4-({4-[(*E*)-2-(2,3,5,6,8,9,11,12-Octahydro-1,4,7,10,13-benzopentaoxacyclopentadecin-15-yl)-1-ethenyl]-1-quinoliniumyl}methyl)-1-benzenesulfonate (4e). Mp: 180−182 °C. ^{1}H NMR (DMSO-d_6): δ 3.64 (m, 8 H, $\gamma,\gamma',\delta,\delta'$-$CH_2O$), 3.81 and 3.85 (m, 4 H, β,β'-CH_2O), 4.16 and 4.23 (2 m, 4 H, α,α'-CH_2O), 6.24 (s, 2 H, CH_2N), 7.11 (d, 1 H, H(C-5′) in benzocrown ether, J = 8.4 Hz), 7.31 (d, 2 H in sulfonatobenzyl), 7.50 (d, 1 H, H(C-6′) in benzocrown ether, J = 8.4 Hz), 7.59 (d, 2 H in sulfonatobenzyl), 7.72 (s, 1 H, H(C-2′) in benzocrown ether), 7.99 and 8.16 (2 m, 2 H, H(C-6), H(C-7) in quinoline), 8.21 (s, 2 H, H(C-a), H(C-b)), 8.34 (d, 1 H in quinoline, J = 9.1 Hz), 8.55 (d, 1 H, H(C-3) in quinoline, J = 6.7 Hz), 9.08 (d, 1 H in quinoline, J = 8.8 Hz), 9.52 (d, 1 H, H(C-2) in quinoline, J = 6.7 Hz). Anal. Calcd for $C_{32}H_{33}NO_8S\cdot 2.5H_2O$: C, 60.36; H, 6.02; N, 2.20. Found: C, 60.31; H, 6.04; N, 2.15.

1-Ethyl-4-[(*E*)-2-(2,3,5,6,8,9,11,12-octahydro-1,4,7,10,13-benzopentaoxacyclopentadecin-15-yl)-1-ethenyl]quinolinium Iodide (4f). A mixture of **9** (1.0 mmol) and **7** (1.2 mmol) was dissolved in 10 mL of anhydrous EtOH, and then 5 mL of pyridine was added. The reaction mixture was heated to reflux for 20 h and concentrated in vacuo. The residue was treated with benzene to remove unreacted **7** and recrystallized successively from MeOH and MeCN to give **4f** in 33% yield. Mp: 136 °C. ^{1}H NMR (DMSO-d_6): δ 1.60 (t, 3 H, Me), 3.65 (s, 8 H, $\gamma,\gamma',\delta,\delta'$-$CH_2O$), 3.82 (m, 4 H, β,β'-CH_2O), 4.15 and 4.22 (2 m, 4 H, α,α'-CH_2O), 5.00 (q, 2 H, CH_2N), 7.10 (d, 1 H, H(C-5′) in benzocrown ether), 7.46 (d, 1 H, H(C-6′) in benzocrown ether), 7.70 (s, 1 H, H(C-2′) in benzocrown ether), 8.05 and 8.25 (2 m, 2 H, H(C-6), H(C-7) in quinoline), 8.15 (d, 2 H, H(C-a), H(C-b), 8.45 (d, 1 H, H(C-3) in quinoline), 8.54 and 9.07 (2 d, 2 H, H(C-5) and H(C-8) in quinoline), 9.32 (d, 1 H, H(C-2) in quinoline). Anal. Calcd for $C_{27}H_{32}NO_5I$: C, 56.16; H, 5.59; N, 2.43. Found: C, 55.96; H, 5.53; N, 2.51.

1-Ethyl-4-[(*E*)-2-(2,3,5,6,8,9,11,12-octahydro-1,4,7,10,13-benzopentaoxacyclopentadecin-15-yl)-1-ethenyl]quinolinium Perchlorate (4g). Compound **4f** (0.03 g, 0.05 mmol) was dissolved with heating in 5 mL of methanol, and then 57% $HClO_4$ (0.09 mL, 0.75 mmol) was added. After cooling, the resulting precipitate was filtered and washed with cold methanol. The yield of **4g** was 0.03 g (95%). The ^{1}H NMR data for **4g** in MeCN-d_3 are given in Table 4.

Synthesis of Cyclobutanes 10a−d. The corresponding styryl dye (i.e., **4a−d**, 0.01 mmol) and $Mg(ClO_4)_2$ (0.011 mmol) were dissolved in 5 mL of anhydrous MeCN. The solution was irradiated with a 405 nm light source; after complete consumption of the dye (monitoring by spectrophotometry), MeCN was evaporated in vacuo. The solid residue was dissolved in a MeCN-d_3/D_2O mixture and analyzed using ^{1}H NMR spectroscopy. The NMR spectra demonstrated that the photolysis afforded cyclobutanes **10a−d** in almost quantitative yields.

2-(4-{2,4-Di(2,3,5,6,8,9,11,12-octahydro-1,4,7,10,13-benzopentaoxacyclopentadecin-15-yl)-3-[1-(2-sulfonatoethyl)-4-quinoliniumyl]cyclobutyl}-1-quinoliniumyl)-1-ethanesulfonate (10a). ^{1}H NMR (MeCN-d_3/D_2O (25%)): δ 3.34 (m, 4 H, 2 $CH_2SO_3^-$), 3.5−3.68 (m, 24 H, 2 $\beta,\beta',\gamma,\gamma',\delta,\delta'$-$CH_2O$), 3.87 (m, 8 H, 2 α,α'-CH_2O), 5.22 (m, 4 H, 2 CH_2N), 5.32 (m, 2 H, cyclobutane H(C-2), H(C-4), $^3J_{H-2,H-3} = {}^3J_{H-1,H-4}$ = 7.7 ± 0.1 Hz, $^3J_{H-1,H-2} = {}^3J_{H-3,H-4}$ = 10.4 ± 0.25 Hz), 5.43 (m, 2 H, cyclobutane H(C-1), H(C-3)), 6.58 (d, 2 H, 2 H(C-5′) in benzocrown ether, $J_{H-5,H-6}$ = 8.4 Hz), 6.76 (d, 2 H, 2 H(C-2′) in benzocrown ether, $J_{H-2,H-6}$ = 2.1 Hz), 6.86 (m, 2 H, 2 H(C-6′) in benzocrown ether, $J_{H-6,H-5}$ = 8.4 Hz, $J_{H-6,H-2}$ = 2.1 Hz), 7.96 (m, 2 H, 2 H(C-6) in quinoline), 8.14 (m, 2 H, 2 H(C-7) in quinoline), 8.22 (d, 2 H, 2 H(C-3) in quinoline, $J_{H-3,H-4}$ = 6.3 Hz), 8.25 (m, 2 H, 2 H(C-8) in quinoline, $J_{H-8,H-7}$ = 8.9 Hz), 8.65 (d, 2 H, 2 H(C-5) in quinoline, $J_{H-5,H-6}$ = 8.4 Hz), 9.17 (d, 2 H, 2 H(C-2) in quinoline, $J_{H-2,H-3}$ = 6.3 Hz).

3-(4-{2,4-Di(2,3,5,6,8,9,11,12-octahydro-1,4,7,10,13-benzopentaoxacyclopentadecin-15-yl)-3-[1-(3-sulfonatopropyl)-4-quinoliniumyl]cyclobutyl}-1-quinoliniumyl)-1-propanesulfonate (10b). ^{1}H NMR (MeCN-d_3/D_2O (10%)): δ 2.35 (m, 4 H, 2 CH_2), 2.75 (m, 4 H, 2 $CH_2SO_3^-$), 3.55−3.75 (m, 24 H, 2 $\beta,\beta',\gamma,\gamma',\delta,\delta'$-$CH_2O$), 3.85 (m, 8 H, 2 α,α'-CH_2O), 5.10 (m, 4 H, 2 CH_2N), 5.31 (m, 2 H, cyclobutane H(C-2), H(C-4), $^3J_{H-2,H-3} = {}^3J_{H-1,H-4}$ = 7.61 ± 0.01 Hz, $^3J_{H-1,H-2} = {}^3J_{H-3,H-4}$ = 10.29 ± 0.01 Hz, $^4J_{H-2,H-4}$ = 0.32 ± 0.02 Hz), 5.42 (m, 2 H, cyclobutane H(C-1), H(C-3), $^4J_{H-1,H-3}$ = 0.49 ± 0.02 Hz), 6.56 (d, 2 H, 2 H(C-5′) in benzocrown ether, $J_{H-5,H-6}$ = 8.4 Hz), 6.81 (d, 2 H, 2 H(C-2′) in benzocrown ether, $J_{H-2,H-6}$ = 1.7 Hz), 6.82 (m, 2 H, 2 H(C-6′) in benzocrown ether, $J_{H-6,H-5}$ = 8.4 Hz, $J_{H-6,H-2}$ = 1.7 Hz), 7.95 (m, 2 H, 2 H(C-6) in quinoline), 8.13 (m, 2 H, 2 H(C-7) in quinoline), 8.26 (d, 2 H, 2 H(C-3) in quinoline, $J_{H-3,H-4}$ = 6.3 Hz), 8.36 (m, 2 H, 2 H(C-8) in quinoline, $J_{H-8,H-7}$ = 9.0 Hz), 8.57 (d, 2 H, 2 H(C-5) in quinoline, $J_{H-5,H-6}$ = 8.5 Hz), 9.20 (d, 2 H, 2 H(C-2) in quinoline, $J_{H-2,H-3}$ = 6.3 Hz). The spin−spin coupling constants for the protons of the benzocrown ether moiety and the cyclobutane ring were obtained by analysis of the spectrum of **10b** in D_2O. The lower coherence of these protons in D_2O and the higher signal:noise ratio provided more precise values of the constants.

4-(4-{2,4-Di(2,3,5,6,8,9,11,12-octahydro-1,4,7,10,13-benzopentaoxacyclopentadecin-15-yl)-3-[1-(4-sulfonatobutyl)-4-quinoliniumyl]cyclobutyl}-1-quinoliniumyl)-1-butanesulfonate (10c). ^{1}H NMR (MeCN-d_3/D_2O (25%)): δ 1.74 (m, 4 H, 2 CH_2 in the tetramethylene chain), 2.09 (m, 4 H, 2 CH_2 in the tetramethylene chain), 2.81 (m, 4 H, 2 $CH_2SO_3^-$, J = 7.6 Hz), 3.5−3.73 (m, 24 H, 2 $\beta,\beta',\gamma,\gamma',\delta,\delta'$-$CH_2O$), 4.12 and 4.16 (m, 8 H, 2 α,α'-CH_2O), 4.93 (m, 4 H, 2 CH_2N, J = 7.6 Hz), 5.33 (m, 2 H, cyclobutane H(C-2), H(C-4), $^3J_{H-2,H-3} = {}^3J_{H-1,H-4}$ = 7.3 ± 0.2 Hz, $^3J_{H-1,H-2} = {}^3J_{H-3,H-4}$ = 10.1 ± 0.2 Hz), 5.42 (m, 2 H, cyclobutane H(C-1), H(C-3)), 6.57 (d, 2 H, 2 H(C-5′) in benzocrown ether, $J_{H-5,H-6}$ = 8.3 Hz), 6.82 (m, 2 H, 2 H(C-6′) in benzocrown ether, $J_{H-6,H-5}$ = 8.3 Hz, $J_{H-6,H-2}$ = 1.9 Hz), 6.84 (d, 2 H, 2 H(C-2′) in benzocrown ether, $J_{H-2,H-6}$ = 1.9 Hz), 7.95 (m, 2 H, 2 H(C-6) in quinoline), 8.13 (m, 2 H, 2 H(C-7) in quinoline), 8.26 (d, 2 H, 2 H(C-3) in quinoline, $J_{H-3,H-4}$ = 6.2 Hz), 8.31 (m, 2 H, 2 H(C-8) in quinoline, $J_{H-8,H-7}$ = 8.9 Hz), 8.66 (d, 2 H, 2 H(C-5) in quinoline, $J_{H-5,H-6}$ = 8.6 Hz), 9.15 (d, 2 H, 2 H(C-2) in quinoline, $J_{H-2,H-3}$ = 6.2 Hz).

2-[(4-{2,4-Di(2,3,5,6,8,9,11,12-octahydro-1,4,7,10,13-benzopentaoxacyclopentadecin-15-yl)-3-[1-(2-sulfonatobenzyl)-4-quinoliniumyl]cyclobutyl}-1-quinoliniumyl)methyl]-1-benzenesulfonate (10d). ^{1}H NMR (MeCN-d_3/D_2O (25%)): δ 3.5−3.88 (2 m, 24 H, 2 $\beta,\beta',\gamma,\gamma',\delta,\delta'$-$CH_2O$), 4.12 and 4.16 (m, 8 H, 2 α,α'-CH_2O), 5.37 (m, 2 H, cyclobutane H(C-2), H(C-4), $^3J_{H-2,H-3} = {}^3J_{H-1,H-4}$ = 7.6 ± 0.1 Hz, $^3J_{H-1,H-2} = {}^3J_{H-3,H-4}$ = 10.6 ± 0.1 Hz, $^4J_{H-2,H-4}$ = 0.2 ± 0.1 Hz), 5.52 (m, 2 H, cyclobutane H(C-1), H(C-3), $^4J_{H-1,H-3}$ = 0.7 ± 0.1 Hz), 6.28 (d, 2 H, 2 H(C-6) sulfonatobenzyl, $J_{H-6,H-5}$ = 7.6 Hz), 6.41 and 6.69 (2 d, 4 H, 2 CH_2N, 2 J_{CHH} = −16.5 Hz), 6.57 (d, 2 H, 2 H(C-5′) in benzocrown ether, $J_{H-5,H-6}$ = 8.3 Hz), 6.82 (m, 2 H, 2 H(C-6′) in benzocrown ether, $J_{H-6,H-5}$ = 8.3 Hz, $J_{H-6,H-2}$ = 1.9 Hz), 6.84 (d, 2 H, 2 H(C-2′) in benzocrown ether, $J_{H-2,H-6}$ = 1.9 Hz), 7.44 (m, 2 H, 2 H(C-4) in sulfonatobenzyl), 7.47 (m, 2 H, 2 H(C-5) in sulfonatobenzyl), 7.90 (m, 2 H, 2 H(C-6) in quinoline), 7.98 (m, 2 H, 2 H(C-7) in quinoline), 8.01 (d, 4 H, 2 H(C-3) in sulfonatobenzyl, $J_{H-3,H-4}$ = 7.8 Hz), 8.28 (m, 2 H, 2 H(C-8) in quinoline, $J_{H-8,H-7}$ = 9.0 Hz), 8.35 (d, 2 H, 2 H(C-

3) in quinoline, $J_{H-3,H-4} = 6.4$ Hz), 8.70 (d, 2 H, 2 H(C-5) in quinoline, $J_{H-5,H-6} = 8.4$ Hz), 9.15 (d, 2 H, 2 H(C-2) in quinoline, $J_{H-2,H-3} = 6.4$ Hz).

Photochemical Measurements. The kinetics of the photoreactions of dyes **4a**−**e** was studied in MeCN solution at ambient temperature. Glass-filtered light of a high-pressure Hg lamp was used for irradiation. The light intensity was measured using a cavity receiver, giving a total error in the quantum yield measurements of about 20%.

The quantum yields of $E \rightarrow Z$ and $Z \rightarrow E$ isomerization for dye **4e** and its metal-complexed form were estimated upon irradiation with 436 or 313 nm light using conventional procedures, since the absorption spectra of both the *E*- and *Z*-isomers of this dye were known.

The quantum yields of PCA and $E \rightarrow Z$ isomerization for **4a**−**d** in $Mg(ClO_4)_2$-containing solutions were measured upon irradiation with 436 nm light. The kinetics of the overall consumption of the *E*-isomer in PCA and $E \rightarrow Z$ isomerization were monitored on the basis of the optical density at 410 nm, where the metal-complexed form of the *E*-isomer showed a much higher absorptivity than did the corresponding photoproducts, i.e., metal-complexed forms of the cycloadduct and the *Z*-isomer.

The kinetics of *E*-isomer conversion to cycloadduct was measured using the four-stage procedure described in the Results and Discussion. Analysis of these two kinetic curves gave the quantum yields of PCA and $E \rightarrow Z$ isomerization. The quantum yields of retrophotocycloaddition for **4a**−**d** were derived from the kinetics of the overall recovery of the dye upon irradiation of the corresponding cycloadducts **10a**−**d** with 313 nm light.

Acknowledgment. This work was supported by the Russian Foundation for Basic Research (RFBR; Grant Number 03-03-32178), the U.S. Civilian Research and Development Foundation (CRDF; Grant Number RC2-137), the U.S. National Science Foundation (NSF; Grant Number CHE-9901213), and the University of Umeå in the framework of a joint project of the University of Umeå and the Photochemistry Center of the Russian Academy of Sciences (CRDF, Grant Number RC0-872).

Supporting Information Available: Analytical methods and 2D NOESY spectra of dimeric complex $\{[(E)\text{-}\mathbf{4b}]\cdot Mg^{2+}\}_2$ and cyclobutane **10d** are available. This material is available free of charge via the Internet at http://pubs.acs.org.

JO034460X